JOURNAL OF ENVIRONMENTAL SCIENCES 72 (2018) 198–207

Available online at www.sciencedirect.com

ScienceDirect

www.elsevier.com/locate/jes

JES JOURNAL OF ENVIRONMENTAL SCIENCES

www.jesc.ac.cn

Characterization of aircraft emissions and air quality impacts of an international airport

Xiaowen Yang[1], *Shuiyuan Cheng*[1,2,*], *Jianlei Lang*[1], *Ran Xu*[3], *Zhe Lv*[1]

1. *Key Laboratory of Beijing on Regional Air Pollution Control, Beijing University of Technology, Beijing 100124, China*
2. *Collaborative Innovation Center of Electric Vehicles in Beijing, Beijing 100081, China*
3. *National Meteorological Center of CMA, Beijing 100081, China*

ARTICLE INFO

Article history:
Received 25 July 2017
Revised 31 December 2017
Accepted 15 January 2018
Available online 3 February 2018

Keywords:
Beijing Capital International Airport
Aircraft
Emission inventory
Air quality

ABSTRACT

Beijing Capital International Airport (ZBAA) is the world's second busiest airport. In this study, the emissions of air pollutants from aircraft and other sources at ZBAA in 2015 were estimated using an improved method, which considered the mixing layer height calculated based on aircraft meteorological data relay (AMDAR), instead of using the height (915 m) recommended by ICAO. The yearly emissions of NO_x, CO, VOCs, SO_2, and $PM_{2.5}$ at the airport were 8.76×10^3, 4.43×10^3, 5.43×10^2, 4.80×10^2, and 1.49×10^2 ton/year, respectively. The spatial–temporal distribution of aircraft emissions was systematically analyzed to understand the emission characteristics of aircraft. The results indicated that NO_x was mainly emitted during the take-off and climb phases, accounting for 20.5% and 55.5% of the total emissions. CO and HC were mainly emitted during the taxi phase, accounting for 91.6% and 92.2% of the total emissions. Because the mixing layer height was high in summer, the emissions of aircraft were at the highest level throughout the year. Based on the detailed emissions inventory, four seasons simulation using WRF-CMAQ model was performed over the domain surrounding the airport. The results indicated that the contribution to $PM_{2.5}$ was relatively high in winter; the average impact was about 1.15 μg/m^3 within a radius of 1 km around the airport. Meanwhile, the near surroundings and southwest areas of the airport are the most sensitive to $PM_{2.5}$.

Introduction

With the development of economy, air transportation plays a significant role in global economic activities and air traffic has increased continuously over the last several decades (Vichi et al., 2016). From 1960 to 2005, global passenger air travel grew from 109 billion to 3.7 trillion passenger-km traveled (Stettler et al., 2011). Depending on a recent report of the Federal Aviation Administration (FAA), the number of passengers in aviation transportation is predicted to grow at an average annual rate of 2.5% by 2036 (FAA, 2016). With the rapid increase in air traffic demand, aircraft emissions as an important source of air pollution, have attracted widespread attentions (Masiol and Harrison, 2015; Stratmann et al., 2016). Aircraft engines produce NO_x, CO, HC, SO_2, CO_2, H_2O, PM and other trace compounds that are primary air pollutants or the precursor of secondary pollutants in the atmosphere (International Civil Aviation Organization (ICAO), 2011). Many studies have shown that air pollutants produced by a large airport could affect air quality near surroundings areas of the airport, even throughout the

* *Corresponding author. E-mail:* chengsy@bjut.edu.cn (Shuiyuan Cheng).

https://doi.org/10.1016/j.jes.2018.01.007
1001-0742/

wider region (Rissman et al., 2013; Hudda and Fruin, 2016). Therefore, the environmental impact of airport emissions is still a significant issue to deal with for air quality management.

During recent years, most studies have been focused on the estimation of aircraft emissions and their impact. For example, Song and Shon (2012) estimated the emissions of greenhouse gases (CO_2, N_2O, CH_4, and H_2O) and air pollutants (NOx, CO, VOCs, and PM) from aircraft at four major international airports in Korea using the Emissions and Dispersion Modeling System (EDMS). Winther et al. (2015) presented an emission inventory of NO_x and PM for aircraft main engines, Auxiliary Power Units (APUs) and handling equipment, which was based on activity data and emission factors for the airport. Simonetti et al. (2015) calculated the total yearly emissions of NOx, CO, SOx, VOCs, and PM_{10} using the EDMS, and analyzed the characteristics of aircraft emissions, and they found that NO_x, SO_x and PM_{10} were mainly emitted during the take-off phases. Carslaw et al. (2012) estimated that the contribution of the emissions of NOx from Heathrow airport was 12–16 $\mu g/m^3$ at Oaks Road, which is a measurement site located at the south boundary of the airport. Song et al. (2015) simulated the impact of aircraft emissions on the O_3 concentration at and around three international airports using WRF-CMAQ model, and they found that aircraft emissions can have a noticeable impact on the concentrations of O_3 and NO_x in the airports and their surrounding areas. Yim and Stettler (2013) assessed the air quality impacts of UK airports using WRF-CMAQ model, and their results showed that more than 65% of the health impacts of UK airports could be reduced by jet fuel desulfurization and improved using GSE and APUs. However, almost all studies on airport emissions inventory estimates have only focused on emissions of aircraft, APU, and ground support equipment. There was little research on other sources of pollution at the airport. Moreover, most of these researches use one of the two methods to quantify aircraft engine emissions, one is using landing and take-off (LTO) cycle to estimate aircraft emissions, another is using the reference values recommended for aircraft emission calculations by the ICAO (2011). The LTO cycle defined by ICAO includes all activities near the airport that takes place below the atmospheric mixing height (altitude of 915 m) while the actual mixing height will change in different times and different locations. Therefore, these two methods that qualified the mixing layer height as 915 m will lead to high uncertainty of the estimation. Detailed and accurate estimations of airport emissions are essential for analyzing the characteristics of air pollutants and examining their impact on the air quality. On the other hand, despite the fact that more and more studies give attentions to aircraft emissions at ground level and air pollution in the vicinity of airports, there are still gaps for these studies, particularly in airports in Asia.

Here we focus on the Beijing Capital International Airport (ZBAA) which is the second busiest airport in the world based on passenger traffic (Airports Council International, 2016). The main aim of this study is to estimate a relatively accurate emission inventory, including the emission of aircraft main engines, APUs, ground support equipment, ground access vehicles, private vehicles, stationary sources, oil depot, and road fugitive dust. The daily changes in the height of the mixing layer are taken into consideration when calculating aircraft emissions. In addition, frequently occurred air pollution problems in Northern China have attracted widespread attention in recent years (Li and Han, 2015; Huang et al., 2015). We quantify the impact of aircraft emissions on regional air quality, especially in regard to $PM_{2.5}$. The obtained results could help government choosing locations of new airports and planning land use near airports, and thus provide the scientific basis for air pollution control in the airport.

1. Materials and methods

ZBAA is the busiest and largest airport in China with three main runways and is located approximately 25 km away from the northeast of the city center (Tiananmen Square) (Fig. 1) (CAAC, 2016). First, a detailed inventory including NO_x, CO, VOCs, SO_2, and $PM_{2.5}$ was calculated for aircraft and other sources in the airport. Then, the impact distribution of these emissions on regional air quality around Beijing was simulated using meteorological and air quality models.

1.1. Aircraft emissions

Aircraft emissions depended on the following factors: the numbers and types of aircraft, types of aircraft engines, fuel used, time spent on each operation phase, power setting, and distance of flight (Song and Shon, 2012). Traditionally, the research of emissions from aircraft and its impact could be generally divided into two parts: aircraft pollutant emissions occurring during the LTO phase (local pollutant emissions), and the non-LTO flight phases (*i.e.*, above 915 m and at cruise level) (ICAO, 2011). The effect of aircraft emissions for human activities at ground level was the most important and all airport related emission source activities were increasing rapidly (Tsilingiridis, 2009). Therefore the emissions of aircraft during the LTO phase were considered, excluding the cruise phase.

1.1.1. Estimation methods

According to standard LTO cycle, aircraft emissions were divided into four activities: taxi emissions occurring on the ground, take-off emissions occurring from 0 m to 304 m for departing planes, climb emissions occurring from 304 m to 915 m for departing planes, and approach emissions occurring from 915 m to 0 m for arriving planes (Rissman et al., 2013). However, the actual mixing height, which determined the time of the approach and climb, will change in different times. Therefore, this approach may result in inaccurate emissions estimation. In this study, we had made improvements to the computing method according to Eqs. (1) to (3) (Kurniawan and Khardi, 2011):

$$E_{ij} = \sum (\mathrm{TIM}_{jk} \times 60) \times (FF_{jk}/1000) \times (EI_{jk}) \times (NE_j) \quad (1)$$

E_{ij} emissions (g) of pollutant i (*e.g.*, NO_x, CO, or HC) for the aircraft type j.

EI_{jk} emission indices (g/kg of fuel) for pollutant i, in mode k (*e.g.*, take-off, climb, taxi, and approach) for each engine used on aircraft type j.

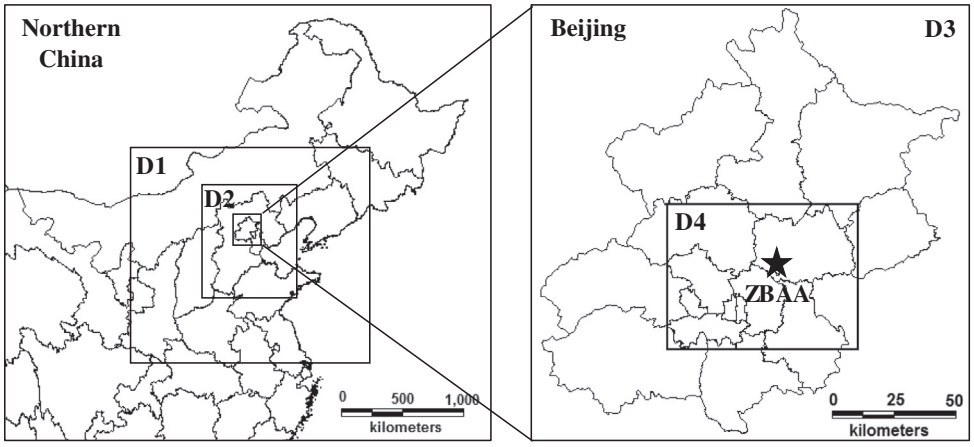

Fig. 1 – The four-level modeling domains and the location of airport in the study area.

FF_{jk} Fuel flow (kg/sec) for mode k, for each engine used on aircraft type j.
TIM_{jk} time-in-mode (min) for mode k for the aircraft type j.
NE_j number of engines used on aircraft type j.

Climb time:

$$TIM_{adj} = TIM_{jk} \times \left(\frac{\text{Mixing height}-304}{915-304}\right) \quad (2)$$

Approach time:

$$TIM_{adj} = TIM_{jk} \times \left(\frac{\text{Mixing height}}{915}\right) \quad (3)$$

TIM_{adj} Adjustments for climb and approach times.

1.1.2. Data preparation

The mixing layer height varies between 500 m and 2000 m with the change of meteorological conditions (Davies et al., 2007). In general, the height of the mixing layer is low in the morning and evening, and reaches the maximum in the afternoon. We set the daily maximum height of the mixing layer as the maximum height of the climb and approach of the aircraft. In this study, aircraft meteorological data relay (AMDAR) was used to draw the morning temperature profile at ZBAA. The daily maximum mixing layer height was calculated by dry adiabatic method which used the morning temperature and the daily maximum ground temperature (Cheng et al., 2002).

The emission inventory used detailed activity data provided by ZBAA, including each aircraft type, origin and destination, estimated time of arrival and actual time of arrival, estimated time of departure and actual time of departure. The average times in a standard LTO cycle were 4 min for approach, 0.7 min for take-off, 2.2 min for climb, and 26 min for taxi (ICAO, 2011). In this study, we used not only the improved models to calculate the time of climb and approach, but also the actual taxiing time of the aircraft using the information obtained from the airport. These data were of great importance for estimating an accurate aircraft emission inventories.

Engine emission indices have been obtained from the ICAO Aircraft Engine Emissions Databank (ICAO, 2016). Matching information between engine and aircraft types was obtained from Stettler et al. (2011) and the engine manufacturer. A complete list of emission indices of various pollutants based on LTO of aircraft is shown in Table S1 of the Supplementary data. The engine databank provides fuel flow rates (kg/sec), engine type (turbofan or multiple turbofan), smoke numbers, and emissions indices for HC, CO, and NO_x. Currently, the engine databank doesn't have the emission indices for SO_2 and $PM_{2.5}$. In this study, emission indices for SO_2 were obtained *via* the methodologies described by Kalivoda (1997). According to the work reported by Unal et al. (2005), the Federal Aviation Administration had created a first-order approximation method to calculate $PM_{2.5}$ emissions from aircraft (Wayson et al., 2003), which related the $PM_{2.5}$ emissions to Smoke Number (SN) and fuel flow rate (FF). The equation for $PM_{2.5}$ emission indices is shown below:

$$EI_{jk} = 0.6 \times (SN_{jk})^{1.8} \times (FF_{jk}) \quad (4)$$

EI_{jk} Emission indices (mg/sec) for $PM_{2.5}$, in mode k (*e.g.*, take-off, climb, taxi, and approach) for each engine used on aircraft type j.
SN_{jk} Smoke Number for mode k for the aircraft type j.
FF_{jk} Fuel flow (kg/sec) for mode k, for each engine used on aircraft type j.

1.2. Other source emissions

Aircraft tends to dominate airport emissions. However, APUs, ground support equipment, and other sources also contribute significantly to overall emissions. Thus, the emissions from aircraft, APUs, and other sources were also taken into account in this study.

APU is a self-contained power unit on an aircraft providing electrical power to ground operating system for aircraft (ICAO,

Table 1 – Operating modes and time of auxiliary power units at Beijing Capital International Airport.

Activity	Mode	Two-engine aircraft	Four-engine aircraft
APU start-up and stabilization	Start-up	3 min	3 min
Aircraft preparation, crew and passenger boarding	Normal running	56.4 min	54.7 min
Main engine start	High load	35 sec	140 sec
Passenger disembarkation and aircraft shutdown	Normal running	15 min	15 min

APU: Auxiliary Power Unit.

2011). APU is different from aircraft main engines which is not certificated for emissions, and the manufacturers wouldn't make the information on APU emission rates public. As a result, there are little data available to calculate APU emissions. Instead, we used the specific times-in-modes provided by the ICAO (ICAO, 2011). Combined with the actual situation of the Beijing Capital International Airport, these times-in-modes are shown in Table 1.

ICAO divided the aircraft types into long-haul and short-haul. The long-haul group included aircraft with a maximum range of more than 8000 km (*e.g.*, A330, A340, A380, B747, B767-200ER, B763, B764, B777, IL96), while the short-haul would include all other kinds of aircraft (ICAO, 2011). The emission factors of APU are given in Table 2.

Other sources in the airport included ground support equipment, ground access vehicles, private vehicles, stationary sources, airport oil depot, and road fugitive dust. The basic data were mainly obtained from the airport and environmental protection bureau. The emissions were calculated based on the categories of activities and their emission coefficients. The detailed descriptions of the methods were according to Cheng et al. (2012) and Lang et al. (2013).

1.3. Model descriptions

In this study, the Weather Research and Forecasting (WRF) and the Models-3/Community Multiscale Air Quality (CMAQ) were respectively used as the meteorological and chemistry-transport air quality models. WRF is a limited-area and non-hydrostatic model which is designed to simulate mesoscale and regional-scale atmospheric circulation (Song et al., 2015). The air quality model CMAQ, which was developed by US EPA, is an Eulerian model based on a 3-D grid. It is a complicated modeling system which can simulate the concentrations of PM, ozone, and other atmospheric pollutants at regional scales (Lang et al., 2013). CMAQ was used in the past to model the impact of aviation emissions (Rissman et al., 2013; Yim and Stettler, 2013; Song et al., 2015).

The WRF model was used for providing the meteorological data required by the CMAQ model. The emission inventory which was another important input data of CMAQ model was divided into two parts. One was a detailed airport emission inventory; another was the county-level air pollutant emission inventory, which was mainly obtained from local environmental protection bureaus or administrations. More detailed information on emission calculation method could be found in former works published by our colleagues (Cheng et al., 2012; Lang et al., 2013; Wen et al., 2016). The entire study area was divided into four domains using a one-way nesting method (Fig. 1). Modeling domain 1 was divided into 57 × 65 grid cells with a spatial resolution of 27 km × 27 km, covering most areas of northeastern China; modeling domain 2 was divided into 90 × 81 grid cells with a spatial resolution of 9 km × 9 km, covering Beijing and its surrounding regions; modeling domain 3 was divided into 60 × 60 grid cells with a spatial resolution of 3 km × 3 km, covering Beijing; modeling domain 4 was divided into 60 × 78 grid cells with a spatial resolution of 1 km × 1 km, covering Beijing Capital International Airport and the urban area of Beijing. Vertically, 35 sigma levels were set in the WRF simulation. The MCIP (Meteorology-Chemistry Interface Processor) was used to transform the formation of the hourly WRF outputs from 35 vertical levels into 14 levels to apply to the CMAQ model. The gas-phase chemistry mechanism was CB05 (Carbon Bond Mechanism).

The time was set as January, April, July, and October in 2015 for modeling to represent winter, spring, summer, and autumn. Two scenarios were used to simulate the impact of the airport on the surrounding area, including the Zero

Table 2 – Emission factors of auxiliary power units.

Aircraft group	Short-haul	Long-haul
Duration of APU operation	45 min	75 min
NOx	700 g	2400 g
HC	30 g	160 g
CO	310 g	210 g

APU: Auxiliary Power Unit.

Table 3 – Emissions at Beijing Capital International Airport in 2015 (ton/year).

Sources	NO_x	CO	VOCs	SO_2	$PM_{2.5}$
Approach	1.07E+03	2.15E+02	1.52E+01[a]	9.76E+01	2.11E+01
Taxi/idle	7.47E+02	3.19E+03	3.38E+02[a]	1.56E+02	1.41E+01
Take-off	1.55E+03	1.32E+01	2.96E+00[a]	4.56E+01	7.34E+00
Climb	4.20E+03	6.51E+01	1.05E+01[a]	1.61E+02	2.90E+01
Total	7.56E+03	3.49E+03	3.66E+02[a]	4.60E+02	7.15E+01
APU	3.85E+02	1.42E+02	2.12E+01	–	–
GSE	3.41E+02	1.89E+02	5.34E+01	9.70E+00	2.43E+01
GAV	3.71E+02	4.03E+02	5.08E+01	2.05E+00	1.98E+01
Private vehicles	1.65E+01	1.93E+02	1.51E+01	–	1.10E−01
Stationary sources	8.45E+01	1.68E+01	1.37E+01	8.64E+00	8.16E+00
Oil depot	–	–	2.26E+01	–	–
Road fugitive dust	–	–	–	–	2.53E+01
Total	8.76E+03	4.43E+03	5.43E+02	4.80E+02	1.49E+02

[a] Derived from HC using a factor of 1.15.

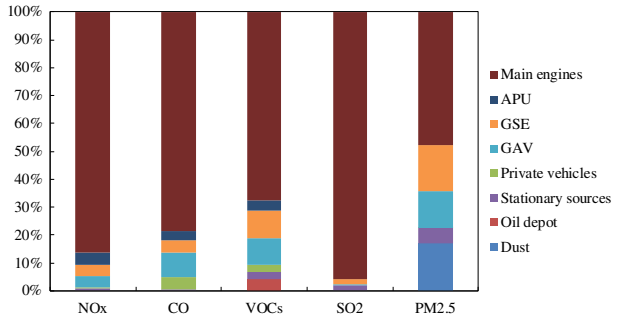

Fig. 2 – Emission contributions of pollution sources at Beijing Capital International Airport in 2015.

Emission Reduction Scenario (ZERS) and the Emission Reduction Scenario (ERS). The ZERS corresponded to the base scenario under which the basic emission inventory, including airport emissions, was used for the WRF-CMAQ model. In terms of the ERS, the emissions from the airport were set to zero. Using the simulation results of ZERS and ERS, the impact of airport emissions can be obtained.

2. Results and discussion

2.1. *Emissions of air pollutants at the airports*

Table 3 presents the emissions of NO_x, CO, VOCs, SO_2, and $PM_{2.5}$ for aircraft main engines, APU, ground support equipment (GSE), ground access vehicles (GAV), private vehicles, stationary sources, airport oil depot, and road fugitive dust at ZBAA in 2015. The yearly emissions of NO_x, CO, VOCs, SO_2, and $PM_{2.5}$ at the airport were 8.76×10^3, 4.43×10^3, 5.43×10^2, 4.80×10^2, and 1.49×10^2 ton/year, respectively. Fig. 2 shows the contributions of different emission sources at ZBAA. Obviously, emission of aircraft was the most important source of all sources in the airport, of which the yearly emissions of NO_x, CO, VOCs, SO_2, and $PM_{2.5}$ were 7.56×10^3, 3.49×10^3, 3.66×10^2, 4.60×10^2, and 7.15×10^1 ton/year, respectively. While those percentages of the on-road mobile sources (GAV and private vehicles), of which the contribution was in the second place, were 4.4%, 13.5%, 12.1%, 0.4%, and 13.4%, respectively. Road fugitive dust was one of the main source of $PM_{2.5}$, the yearly emissions was 25 ton/year, accounting for 17.0% of the total emissions. SO_2 mainly comes from the fuel combustion, so there were some pollutants come from stationary sources. However, compared with aircraft emissions, the contribution of stationary sources was small, less than 2%. The sources of VOCs were more dispersed, such as incomplete combustion of fuel, volatilization of the oil depot and so on. Therefore, in order to control the emissions of airport, different control measures should be carried out for the main sources of different pollutants.

Using the same data on the activity of the Beijing Capital International Airport, we chose to use the reference values recommended for aircraft emissions calculations by the ICAO. The comparison between the results of the improved method (IM) and the standard method (SM) is shown in the Fig. 3. As can be seen from the results, the emissions of NO_x, SO_2, and $PM_{2.5}$ that were calculated by the improved method were obviously higher than the standard method, increasing by 24.0%, 18.6%, and 24.1%, respectively. The difference between those two methods was mainly in the climb and approach phases. While there was a small difference of the emissions of CO and HC calculated by the two methods (less than 3%). This analysis suggests that the uncertainty in NO_x, SO_2, and $PM_{2.5}$ emissions causing by the variations of the height of the mixing height is very large.

The information of the emissions at other airports in former studies was scarce, so we only chose the emissions of aircraft main engines to compare with Beijing Capital International Airport. Table 4 presents the results of the comparison. As indicated in Table 4, even if the number of LTO cycles was about 2/3 of Atlanta International Airport, the emissions of NOx, SO_2 and $PM_{2.5}$ were not proportional of this ratio, NOx emissions were about 1.5 times at Beijing Airport. Mainly because of this approach move part of the emissions currently considered as due to cruise, to the LTO cycle. In general, aircraft emissions correspond to airport LTO cycles, showing that the difference of

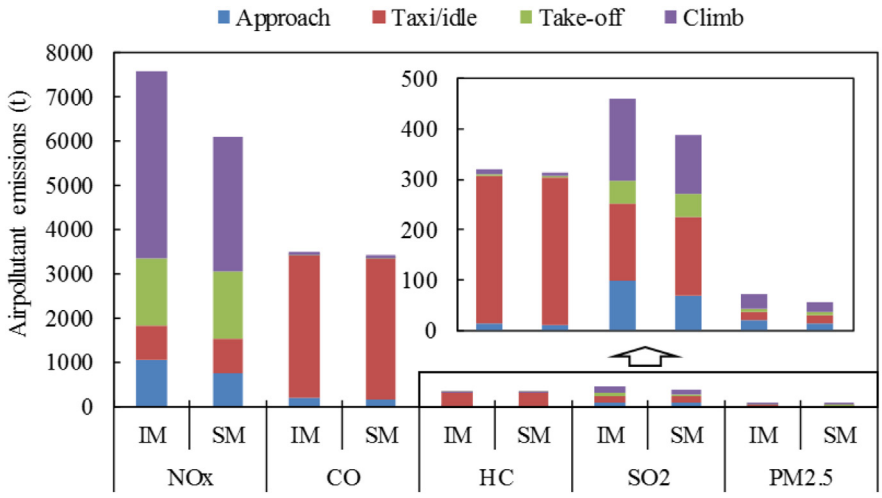

Fig. 3 – The comparison of the improved method (IM) with the standard method (SM).

Table 4 – Aircraft emissions at Beijing Capital International Airport in 2015 compared with other airports (ton/year).

Airport	Time	LTO cycle	NO_x	CO	HC	SO_2	$PM_{2.5}$	Reference
Beijing	2015	295,100	7.56E+03	3.49E+03	3.18E+02	4.60E+02	7.15E+01	This study
Atlanta	2000	423,423	4.91E+03	5.20E+03	8.81E+02 [a]	4.73E+02	7.00E+01	Unal et al. (2005)
Incheon	2010	214,835	3.65E+03	1.75E+03	2.73E+02 [a]	–	1.82E+01 [b]	Song and Shon (2012)
Gimpo		118,514	7.86E+02	1.04E+03	1.62E+02 [a]	–	7.10E+00 [b]	
Gimhae		62,225	3.32E+02	5.70E+02	9.04E+01 [a]	–	3.50E+00 [b]	
Jeju		103,426	6.00E+02	8.84E+02	1.36E+02 [a]	–	5.90E+00 [b]	
Ataturk	2001	160,901	1.26E+03	2.08E+03	3.72E+02	6.66E+01	–	Kesgin (2006)
Antalya		62,443	4.98E+02	7.73E+02	1.07E+02	2.51E+01	–	
Esenboga		43,364	2.19E+02	3.90E+02	7.33E+01	1.21E+01	–	

[a] Derived from VOC using a factor of $(1.15)^{-1}$.
[b] The emissions of PM.

aircraft emissions at different airports was mainly due to the use of different estimation methods (Winther et al., 2015).

2.2. Characteristics of aircraft emissions

2.2.1. The spatial distribution of aircraft emissions

Fig. 4 shows the emission contribution rates of different operation modes at Beijing Capital International Airport. By analyzing the relationship between aircraft emissions and aircraft operation modes, it was found that there were significant differences on the emission rates of different pollutants in different working modes. NO_x was mainly emitted during the climb phase, accounting for 55.5% of the total emissions. The phases of approach, taxi, and take-off accounted for 14.1%, 9.9%, and 20.5% of the total emissions, respectively. Some studies have shown that the emissions indices of NO_x for aircraft engines are positively correlated to thrust setting (Stettler et al., 2011). Therefore, emissions of NO_x were significant in the high thrust operation mode of the aircraft during the phases of take-off and climb. This also explained why the take-off phase only ran for 0.7 min, while the emissions of NO_x accounted for as much as 20.5% of total emissions. Emission characteristics of $PM_{2.5}$ were similar to NO_x, while the emission contribution rates were more evenly distributed. The emissions during approach, taxi, take-off, and climb phases accounted for 29.5%, 19.8%, 10.3%, and 40.5% of the total emissions, respectively. CO and HC were mainly emitted during the taxi phase, accounting for 91.6% and 92.2% of the total emissions. The emission indices of CO and HC decreased with increasing thrust. Thus, in a low thrust environment, the

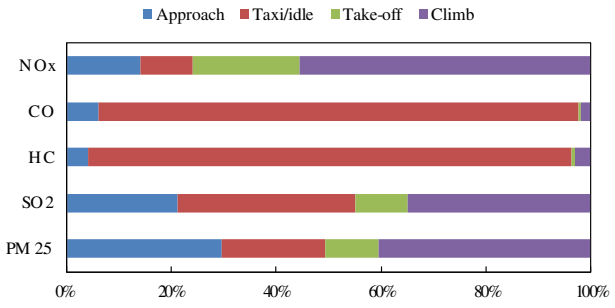

Fig. 4 – Emission contribution rates of different operation modes at Beijing Capital International Airport.

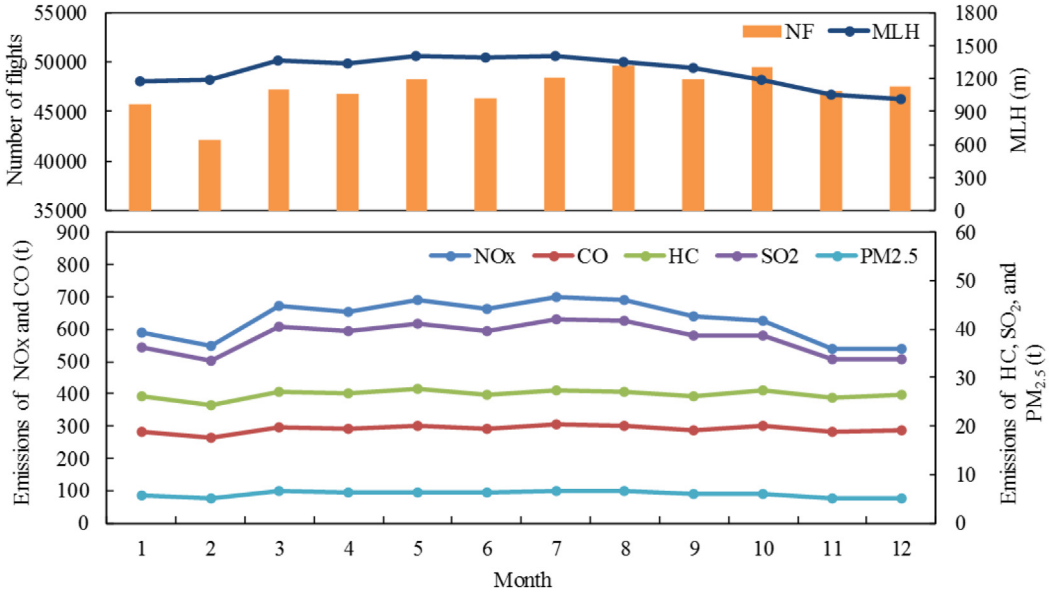

Fig. 5 – Monthly variations in emissions of air pollutants, number of flights (NF), and mixing layer height (MLH).

Table 5 – Comparison of monitored data with simulated results (24-h average $PM_{2.5}$ concentrations).

Season	Monitor	Simulation	NMB	NME	RC
Spring	70.2	55.6	−19.8%	34.2%	77.1%
Summer	59.2	48.2	−16.7%	31.1%	81.2%
Autumn	85.4	76.2	−14.3%	30.8%	82.7%
Winter	95.4	87.1	−16.0%	27.5%	84.8%

pressure and temperature of engine combustion chamber were relatively low which could lead to incomplete combustion of fuel and increasing emissions of CO and HC. On the contrary, as the thrust of the engine increased, the emissions of CO and HC would be significantly reduced. CO and HC emissions during take-off and climb phases accounted for 0.4% to 2.9% of the total emissions. The emissions of SO_2 depend on the fuel consumption and the fuel sulfur content, and the emissions during approach, taxi, take-off, and climb phases accounted for 21.2%, 33.8%, 9.9%, and 35.0% of the total emissions, respectively.

2.2.2. The temporal distribution of aircraft emissions

Fig. 5 presents the monthly variations in emissions of air pollutants, number of flights, and the height of mixing layer. The monthly emissions of air pollutants showed the highest values in July and the lowest in February. The emissions of aircraft were mainly affected by the number of flights and the time of each operation mode. Because of the huge passenger volume of Beijing Capital International Airport, most of the flights have a fixed time and line. Therefore, there will be no significant changes in the number of daily flights. The number of days per month would have a direct impact on the overall number of flights. In addition, the solar radiation in winter (January, February, and December) in Beijing was quite weak, resulting in a lower height of mixing layer. So the time of the aircraft during the climb and approach phases is relatively short, also the emissions of air pollutants were at the lowest level throughout the year. The percentages of NO_x, CO, HC, SO_2, and $PM_{2.5}$ from aircraft main engines in winter accounted for 22.2%, 23.9%, 24.1%, 22.6%, and 22.3% of annual emissions, respectively. Opposite to winter, the solar radiation was strong and the height of mixing layer was high in summer (June, July, and August). So the emission of air pollutants was at the highest level throughout the year, accounting for 27.2%, 25.7%, 25.5%, 26.9%, and 27.0% of annual emissions, for NO_x, CO, HC, SO_2, and $PM_{2.5}$ respectively. Due to the fact that NO_x was mainly emitted during the climb phase, its emission was greatly affected by the height of the mixing layer, and there was a relatively significant variation (9.3% of the mean) in

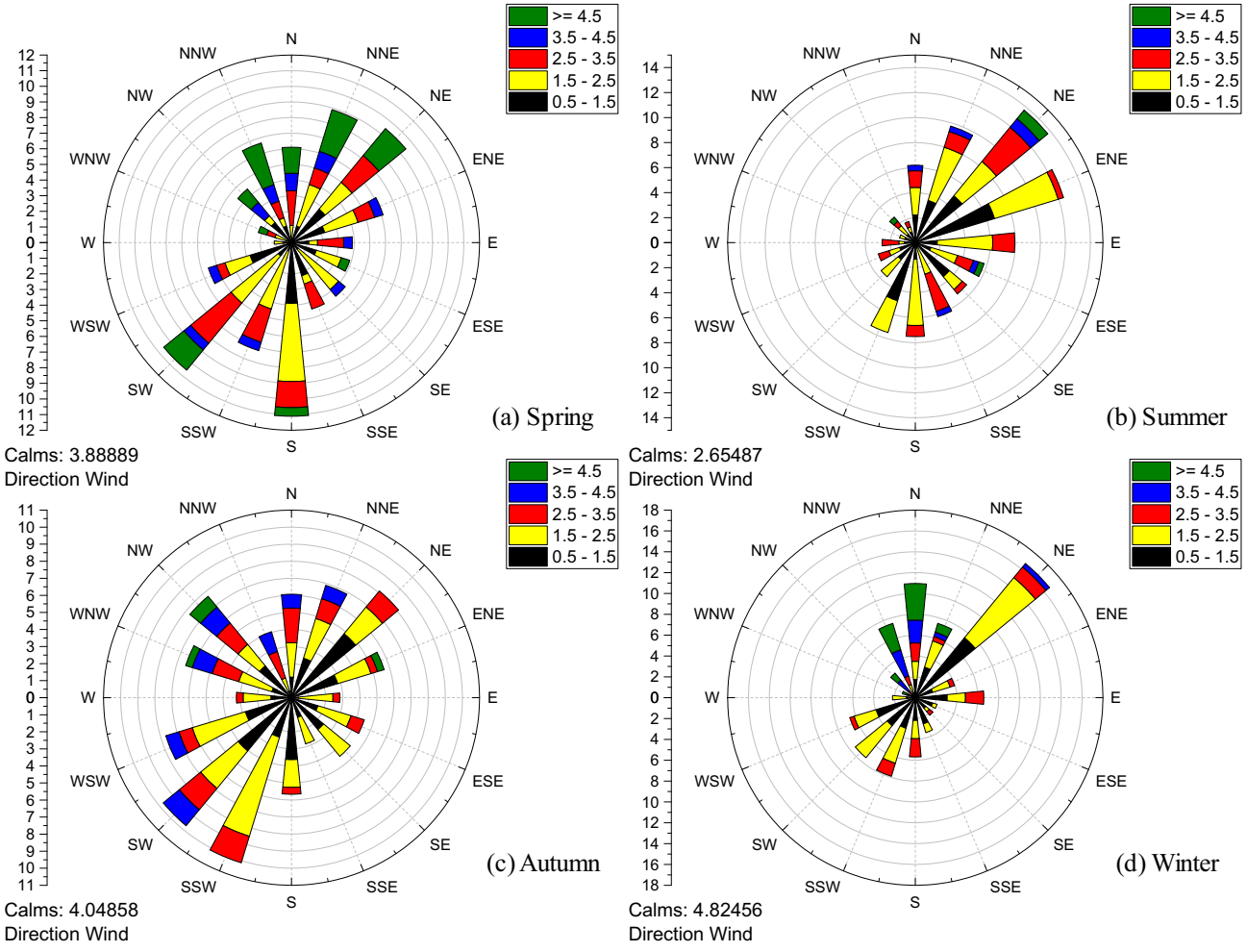

Fig. 6 – The wind rose in spring (a), summer (b), autumn (c), and winter (d) in 2015.

each monthly emission. CO and HC were mainly emitted during the taxi phase, so its emission was irrelevant to the height of the mixing layer. So there was no significant variation (<4% of the mean) in each monthly emission.

2.2.3. *Uncertainty analysis*

In the current methodology for aircraft emission estimation, there were three main sources of uncertainties. Firstly, the daily maximum height of mixing layer was calculated by dry adiabatic method, which was used to determine the height of aircraft emissions. There might be a deviation of the height of mixing layer from the real atmosphere. Secondly, because of the lack of localized aircraft engine emission indices, most of the engine emission indices used in this study were obtained from the ICAO Aircraft Engine Emissions Databank. However, emission indices were the engine test data at sea level static conditions and 7%, 30%, 85%, and 100% of the rated thrust setting. In the actual flight process, the emission indices were not the same as the ideal values due to in-flight condition, aging of the engine, and maintenance. Therefore, there were uncertainties of these emission indices. Thirdly, for estimating other sources of pollution at airports, including ground support equipment, ground access vehicles, private vehicles, stationary sources, airport oil depot, and road fugitive dust, there were uncertainties due to the large number of parameters involved.

2.3. *Impact of airport emissions*

In this study, the normalized mean bias (NMB), normalized mean gross error (NME), and correlation coefficient (RC) were used to assess the accuracy of the CMAQ simulation (USEPA, 2007). The average simulated concentration of $PM_{2.5}$ within the domain 4 containing ten monitoring stations was calculated to compare with the average observed results. Table 5 presents the model verification results in four seasons. Considering the inherent uncertain nature of meteorological and air quality simulation, the modeling performance was acceptable for the WRF-CMAQ to simulate the concentrations of $PM_{2.5}$ in Beijing Capital International Airport and its surrounding regions.

The wind rose of four seasons in 2015 is presented in Fig. 6. The figures show that the wind direction of the airport area was obviously different in the four seasons, and the dominant winds were northeast and southwest. Fig. 7 shows the airport impact on average ground level concentrations of $PM_{2.5}$ in four seasons in 2015 from WRF-CMAQ model. Though each hour of sensitivity was calculated and analyzed, only the average grid sensitivity was shown here. As indicated in Fig. 7, the impact of airport emissions to surrounding areas differed in four seasons. Generally, the concentration distribution of $PM_{2.5}$ was affected by the seasonal dominant wind direction. In spring, $PM_{2.5}$ mainly affected the near surroundings and the western regions of the airport, the impact to the east was relatively small (Fig. 7a). In the vicinity of airport within 1 km, the average contribution of $PM_{2.5}$ was 0.52 $\mu g/m^3$, and the hourly maximum contribution of $PM_{2.5}$ was 4.16 $\mu g/m^3$ in the northwest of the airport, accounting for 11.7% of the grid cell $PM_{2.5}$ concentration. While in the vicinity of airport within 5 km, the average was 0.18 $\mu g/m^3$, and the hourly maximum was 3.37 $\mu g/m^3$ to the west of the airport, accounting for 7.8%. The distribution of $PM_{2.5}$ contributions in autumn was similar

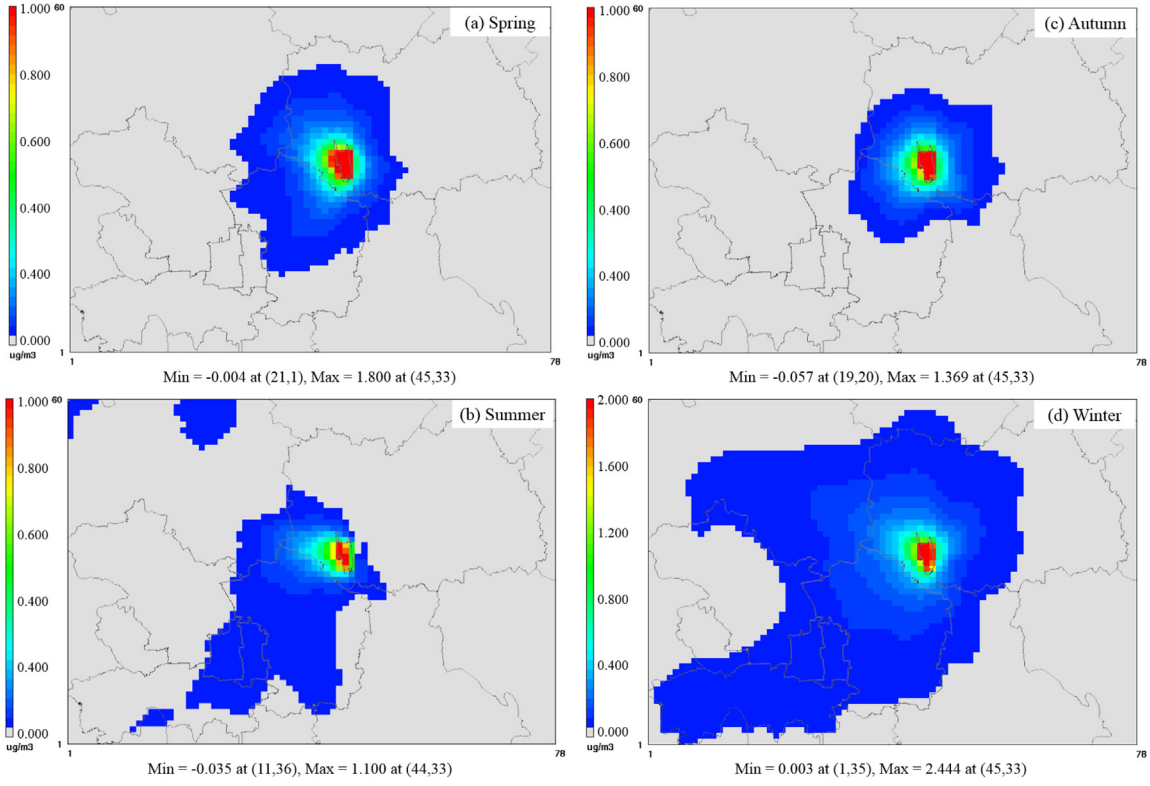

Fig. 7 – Airport impact on average ground level concentrations of $PM_{2.5}$ in spring (a), summer (b), autumn (c), and winter (d) in 2015.

to that in spring, which was mainly affected at the surrounding areas of the airport (Fig. 7c). The average contribution was 0.61 μg/m^3 and the hourly maximum contribution was 6.57 μg/m^3 in the southwest of the airport, in the vicinity of airport within 1 km. While the average contribution and the maximum contribution of $PM_{2.5}$ was 0.21 and 6.92 μg/m^3, respectively, in the vicinity of airport within 5 km. That maximum contribution occurred to the west of the airport, which accounted for 6.5% of the grid cell $PM_{2.5}$ concentrations. In addition, there was a slight decrease in $PM_{2.5}$ contributions to the south and east of the airport, probably due to the reduction in the oxidation of NO_2 as increased NO_x consume O_3 and OH (Unal et al., 2005).

The distribution of $PM_{2.5}$ contributions in summer was quite different from spring and autumn, which was affected in the southern and southwestern regions of the airport, and little in the northeastern (Fig. 7b). In addition, the northwest of the airport was also sensitive to $PM_{2.5}$. The concentration of $PM_{2.5}$ in summer was low, and the $PM_{2.5}$ of airport emissions impact on the surrounding area was relatively small. In the vicinity of airport within 1 km, the average contribution of $PM_{2.5}$ was 0.41 μg/m^3, and the hourly maximum contribution was 3.06 μg/m^3 to the southwest of the airport, which accounted for 13.8% of the grid cell $PM_{2.5}$ concentration. While in the vicinity of airport within 5 km, the average, the hourly maximum and the proportion became 0.10 μg/m^3, 2.37 μg/m^3 and 16.0%. The concentration of $PM_{2.5}$ was relatively high in winter, covering most of the urban areas of Beijing, which was affected by the stable meteorological conditions (Fig. 7d). The impact was higher to the west and southwest of the airport compared to the east and north. In the vicinity of airport within 1 km, the average contribution of $PM_{2.5}$ was 1.15 μg/m^3, while the hourly maximum contribution was 6.61 μg/m^3 to the west of the airport, accounting for 7.6% of the grid cell $PM_{2.5}$ concentrations. When expanding the influence distance to 5 km, the average contribution of $PM_{2.5}$ was 0.45 μg/m^3, and the hourly maximum was 5.37 μg/m^3 in the west of the airport, accounting for 6.2% of the grid cell $PM_{2.5}$ concentrations.

Comprehensive analyses of the above, the near surrounding and northwest areas of the airport are the most sensitive to $PM_{2.5}$, and the emissions of the airport in winter have the greatest impact on the surrounding area.

3. Conclusions

In this study, a detailed emission inventory, including the emission of aircraft main engines, APUs, ground support equipment, ground access vehicles, private vehicles, stationary sources, airport oil depot, and road fugitive dust were calculated at Beijing Capital International Airport. An improved method that considered the daily changes in the height of the mixing layer was used to estimate the aircraft emissions. The yearly emissions of NO_x, CO, VOCs, SO_2, and $PM_{2.5}$ at the airport are 8.76×10^3, 4.43×10^3, 5.43×10^2, 4.80×10^2, and 1.49×10^2 ton/year, respectively. The aircraft was the main source of the airport, of which the emissions of NO_x, CO, VOCs, SO_2, and $PM_{2.5}$ accounted for 86.3%, 78.7%, 67.4%, 95.6%, and 48.0% of total emissions, respectively. By analyzing the characteristics of aircraft emissions, it was found that NO_x was mainly emitted during the take-off and climb phases, accounting for 20.5% and 55.5% of the total emissions. Taxiing aircrafts are a significant source of CO and HC emissions, which accounted for 91.6% and 92.2% of the total emissions. The height of the mixing layer is higher in summer, so the emissions of air pollutants were at the highest level throughout the year. The percentages of NO_x, CO, HC, SO_2, and $PM_{2.5}$ from aircraft accounted for 27.2%, 25.7%, 25.5%, 26.9%, and 27.0% of annual emissions, respectively.

Based on the detailed emission inventory, four-season simulation using WRF-CMAQ model was performed over the domain surrounding the airport. Two scenarios were used to simulate the impact of the airport on the surrounding area, including the zero emission reduction scenario and the emission reduction scenario. The simulation results are shown that the concentration of $PM_{2.5}$ was relatively high in winter, covering most of the urban areas of Beijing, which was affected by the stable meteorological conditions. The average impact was about 1.15 μg/m^3 within a radius of 1 km around the airport. The hourly maximum contribution was 6.61 μg/m^3 in the west of the airport. Generally, the near surrounding and southwest areas of the airport were the most sensitive to $PM_{2.5}$.

Acknowledgments

This work was supported by the Ministry of Science and Technology of China (2016YFC0202705) and the National Natural Science Foundation of China (Nos. 91544232, 51638001). In addition, we greatly appreciated the fund support from Beijing Municipal Commission of Science and Technology (Nos. Z161100004516013, Z171100002217002). The authors are grateful to the anonymous reviewers for their insightful comments.

Appendix A. Supplementary data

Supplementary data to this article can be found online at https://doi.org/10.1016/j.jes.2018.01.007.

REFERENCES

Airports Council International, 2016. Air traffic figures. http://www.aci.aero.

Carslaw, D.C., Williams, M.L., Barratt, B., 2012. A short-term intervention study impact of airport closure due to the eruption of Eyjafjallajökull on near-field air quality. Atmos. Environ. 54, 328–336.

Cheng, S., Jin, Y., Liu, L., Huang, G., Hao, R., Jasson, C.R., 2002. Estimation of atmospheric mixing heights over large areas using data from airport meteorological stations. J. Environ. Sci. Health. Part A 37 (6), 991–1007.

Cheng, S., Zhou, Y., Li, J., Lang, J., Wang, H., 2012. A new statistical modeling and optimization framework for establishing high-resolution PM10 emission inventory — I. Stepwise regression model development and application. Atmos. Environ. 60, 613–622.

Civil Aviation Administration of China (CAAC), 2016. http://www.caac.gov.cn.
Davies, F., Middleton, D.R., Bozier, K.E., 2007. Urban air pollution modelling and measurements of boundary layer height. Atmos. Environ. 41 (19), 4040–4049.
Federal Aviation Administration (FAA), 2016. Aerospace Forecast. https://www.faa.gov/data_research/aviation/aerospace_forecasts/media/FY2016-36_FAA_Aerospace_Forecast.pdf.
Huang, W., Fan, H., Qiu, Y., Cheng, Z., Qian, Y., 2015. Application of fault tree approach for the causation mechanism of urban haze in Beijing—considering the risk events related with exhausts of coal combustion. Sci. Total Environ. 544, 1128–1135.
Hudda, N., Fruin, S.A., 2016. International airport impacts to air quality: size and related properties of large increases in ultrafine particle number concentrations. Environ. Sci. Technol. 50 (7), 3362–3370.
International Civil Aviation Organization (ICAO), 2011. Airport Air Quality Manual. International Civil Aviation Organization.
International Civil Aviation Organization (ICAO), 2016. Aircraft Engine Emissions Databank. http://www.easa.europa.eu/document-library/icao-aircraft-engine-emissions-databank.
Kalivoda, M.T., 1997. Methodologies for Estimating Emissions from Air Traffic—Future Emissions. Meet Project.
Kesgin, U., 2006. Aircraft emissions at Turkish airports. Energy 31 (2), 372–384.
Kurniawan, J.S., Khardi, S., 2011. Comparison of methodologies estimating emissions of aircraft pollutants, environmental impact assessment around airports. Environ. Impact Assess. Rev. 31 (3), 240–252.
Lang, J., Cheng, S., Li, J., Chen, D., Zhou, Y., Wei, X., et al., 2013. A monitoring and modeling study to investigate regional transport and characteristics of $PM_{2.5}$ pollution. Aerosol Air Qual. Res. 13 (3), 943–956.
Li, J., Han, Z., 2015. A modeling study of severe winter haze events in Beijing and its neighboring regions. Atmos. Res. 170, 87–97.
Masiol, M., Harrison, R.M., 2015. Quantification of air quality impacts of London Heathrow Airport (UK) from 2005 to 2012. Atmos. Environ. 116, 308–319.
Rissman, J., Arunachalam, S., Woody, M., West, J.J., BenDor, T., Binkowski, F.S., 2013. A plume-in-grid approach to characterize air quality impacts of aircraft emissions at the Hartsfield-Jackson Atlanta International Airport. Atmos. Chem. Phys. Discuss. 13 (18), 9285–9302.
Simonetti, I., Maltagliati, S., Manfrida, G., 2015. Air quality impact of a middle size airport within an urban context through EDMS simulation. Transport. Res. D-TR. E. 40, 144–154.
Song, S.-K., Shon, Z.-H., 2012. Emissions of greenhouse gases and air pollutants from commercial aircraft at international airports in Korea. Atmos. Environ. 61 (61), 148–158.
Song, S.-K., Shon, Z.-H., Kang, Y.-H., 2015. Comparison of impacts of aircraft emissions within the boundary layer on the regional ozone in South Korea. Atmos. Environ. 117, 169–179.
Stettler, M.E.J., Eastham, S., Barrett, S.R.H., 2011. Air quality and public health impacts of UK airports. Part I: emissions. Atmos. Environ. 45 (31), 5415–5424.
Stratmann, G., Ziereis, H., Stock, P., Brenninkmeijer, C.A.M., Zahn, A., Rauthe-Schoch, A., et al., 2016. NO and NOy in the upper troposphere: nine years of CARIBIC measurements onboard a passenger aircraft. Atmos. Environ. 133, 93–111.
Tsilingiridis, G., 2009. Aircraft air pollutant emissions in Greek airports. Global Nest J. 11 (4), 528–534.
U.S. Environment Protection Agency, 2007. EPA-454/B-07-002. Guidance on the Use of Models and Other Analyses for Demonstrating Attainment of Air Quality Goals for Ozone, PM2.5, and Regional Haze.
Unal, A., Hu, Y., Chang, M.E., Odman, M.T., Russel, A.G., 2005. Airport related emissions and impacts on air quality: application to the Atlanta International Airport. Atmos. Environ. 39 (32), 5787–5798.
Vichi, F., Frattoni, M., Imperiali, A., Balducci, C., Cecinato, A., Perilli, M., et al., 2016. Civil aviation impacts on local air quality: a survey inside two international airports in central Italy. Atmos. Environ. 142, 393–405.
Wayson, R.L., Fleming, G.G., Kim, B., 2003. Status Report on Proposed Methodology to Characterize Jet/Gas Turbine Engine Particulate Matter Emissions. US Department of Transportation, Federal Aviation Administration.
Wen, W., Cheng, S., Chen, X., Wang, G., Li, S., Wang, X., et al., 2016. Impact of emission control on PM2.5 and the chemical composition change in Beijing-Tianjin-Hebei during the APEC summit 2014. Environ. Sci. Pollut. Res. 23, 4509–4521.
Winther, M., Kousgaard, U., Ellermann, T., Massling, A., Nojgaard, J.K., Ketzel, M., 2015. Emissions of NOx, particle mass and particle numbers from aircraft main engines, APU's and handling equipment at Copenhagen Airport. Atmos. Environ. 100, 218–229.
Yim, S.H.L., Stettler, M.E.J., 2013. Barrett S R H. Air quality and public health impacts of UK airports. Part II: impacts and policy assessment. Atmos. Environ. 67 (67), 184–192.